SPECIAL ISSUE

CHILDREN'S READING PERFORMANCE IS CORRELATED WITH WHITE MATTER STRUCTURE MEASURED BY DIFFUSION TENSOR IMAGING

Gayle K. Deutsch[1*], Robert F. Dougherty[1], Roland Bammer[2], Wai Ting Siok[1], John D.E. Gabrieli[1] and Brian Wandell[1]

([1]Department of Psychology, Stanford University, Stanford, CA, USA; [2]Department of Radiology, Stanford University, Stanford, CA, USA)

ABSTRACT

We investigated the white matter structure in children (n = 14) with a wide range of reading performance levels using diffusion tensor imaging (DTI), a form of magnetic resonance imaging. White matter structure in a left temporo-parietal region that had been previously described as covarying with reading skill in adult readers also differs between children who are normal and poor readers. Specifically, the white matter structure measured using fractional anisotropy (FA) and coherence index (CI) significantly correlated with behavioral measurements of reading, spelling, and rapid naming performance. In general, lower anisotropy and lower coherence were associated with lower performance scores. Although the magnitude of the differences in children are smaller than those in adults, the results support the hypothesis that the structure of left temporo-parietal neural pathways is a significant component of the neural system needed to develop fluent reading.

Key words: diffusion tensor imaging, white matter, reading, dyslexia

INTRODUCTION

Adult reading skill spans a wide performance range across individuals. This variance in performance begins in childhood. Educational opportunity, the stress and distractions associated with low SES, and many other socio-cultural factors clearly play an important role in the development of fluent reading (Adams, 1990). Individual psychological issues also play a role - a child must be motivated and have some degree of emotional stability in order to learn a complex skill such as reading. But many individuals with adequate intelligence struggle to learn to read despite high motivation and sufficient opportunity. At present an estimated 5% to 17% of English-speaking children are diagnosed with dyslexia characterized as a difficulty learning to read with no apparent cause (Shaywitz, 1998). This observation, coupled with results of genetic linkage analyses (see Grigorenko, 2001 for a review) and low-level perceptual deficits related to reading (see Stein, 2001 for a review), has led to the hypothesis that certain brain phenotypes may be less adapted to the acquisition of fluent reading. There is considerable value, then, in identifying quantitative measures of brain anatomy that can be used to predict the degree of difficulty an individual may have in acquiring fluent reading performance. These measures may provide objective diagnoses of reading disability, and they will illuminate the mechanisms of reading acquisition in general.

Based on a wide variety of measurements, there is now broad agreement that disruption of neural pathways located in left temporo-parietal cortex is associated with poor reading (see Habib, 2000; Temple, 2002 for reviews). Postmortem studies of dyslexics, for example, have indicated cellular anomalies (ectopias and dysplasia) in the left perisylvian region (Galaburda et al., 1985). Functional measurements using positron emission tomography (PET) and functional magnetic resonance imaging (fMRI) show differences between adult dyslexics and normal controls in left temporo-parietal brain regions (Brunswick et al., 1999; Paulesu et al., 1996, 2001; Rumsey, 1992; Rumsey et al., 1997; Shaywitz et al., 1998). During reading and phonological processing tasks dyslexics generally have reduced left temporo-parietal responses relative to controls. Recent fMRI studies have identified similar differences in children (Temple et al., 2001; Shaywitz et al., 2002). On the basis of magnetic source imaging (MSI) results, Simos et al. (2000a, 2000b) have suggested that these neural pathways in the left temporo-parietal cortex are essential for the development of skilled reading.

Diffusion Tensor Imaging (DTI)

In this report, we describe new measurements that evaluate an association between reading performance and the structure of white matter tracts in the developing child's brain. To assess the white matter structure, we used diffusion tensor imaging (DTI), a relatively recent neuroimaging method that measures the diffusion of water molecules in brain tissue (Le Bihan et al., 2001; Hunsche et al., 2001; Bammer et al., 2002). DTI also provides information about the direction of diffusion, which can be used to infer alignment and coherence of white matter axons in many regions of the brain. This is a fundamentally different measurement of brain tissue compared to conventional magnetic resonance imaging. Specifically, conventional anatomical imaging is

excellent at discriminating white matter from gray matter. However, it is poor at discriminating the fine tissue structure within the white matter. DTI allows one to discriminate between regions within white matter based on differences in the pattern of diffusion within white matter structures. Further, DTI can be used to quantitatively compare the integrity of the same white matter region across subjects. For example, DTI can be used to differentiate white matter regions that contain many aligned myelinated axons from regions with crossing axons, less myelination, or less coherently organized arrays of axons. Four important properties of brain tissue can be derived from the DTI measurements: isotropic diffusion coefficient (i.e. Trace), fractional anisotropy (FA), fiber direction, and coherence index (CI). The isotropic diffusion coefficient expresses an overall effect of diffusion change and provides complementary information to changes in diffusion anisotropy. FA values are a measure of microstructural features within a voxel and reflect the orientation-dependence of diffusion; high FA values within a voxel suggest the presence of highly directional diffusion such as that seen in white matter fiber tracts. The principal diffusion direction can be estimated for each voxel and, given a priori assumptions of the restricted diffusion perpendicular to the nerve fibers, this permits an estimation of the principal fiber direction within the voxel. Finally, DTI measurements can also be used to estimate the overall orientation coherence of fibers in adjacent voxels (CI). A high CI value indicates both the local strength of FA and the agreement of fiber direction in neighboring voxels.

In a study emphasizing the anatomical difference between controls and reading impaired adults, Klingberg et al. (2000) compared FA and CI values. They found reliable differences in FA in the temporo-parietal region bilaterally, but more extreme differences in the left hemisphere. Furthermore, FA values in the left temporo-parietal lobe correlated with reading performance in both poor and normal readers. Although group differences in CI were not observed, quantification of the fiber direction revealed that a slight preponderance of axons in the left temporo-parietal region were oriented in an anterior-posterior direction. They suggested that axons in this area are important for efficient connectivity between temporo-parietal and frontal regions and thus may be important for reading.

The current study was designed to investigate whether the anatomical differences seen in the DTI measurements in adults are present in children at an age when reading skills are rapidly developing. White matter structural differences in FA and/or CI between poor and normal reading children would support the premise that neural pathways in this brain region are fundamental to reading development rather than the alternate hypothesis that many years of differential reading experiences cause the structural discrepancy reported in adults.

Materials and Methods

Subjects

Subjects (n = 14) were children with English as their primary language. Written informed consent was obtained from all subjects (with their parents) before participating. The Stanford Panel on Human Subjects in Medical and Non-Medical Research approved all procedures. Children were recruited from the local community and all subjects were physically healthy and had no history of neurological disease, head injury, attention deficit/hyperactivity disorder or psychiatric disorder. Children were between 7-13 years of age. All children were strongly right-handed, as assessed by the Edinburgh Handedness Inventory (Oldfield, 1971), except for one child in the poor reading group. Although the handedness quotient (HQ) suggests that this child is weakly right-handed (HQ = 40) she uses only her right hand for writing. The subjects' characteristics are listed in Table I. There were no significant group differences for age, gender, HQ, parental education, socioeconomic status (SES) using the Hollingshead Inventory (Hollingshead, 1975) or Full-Scale IQ (FSIQ). FSIQ was obtained by pro-rated Verbal IQ and Performance IQ scores from the Wechsler Intelligence Scale for Children-III (WISC-III) (Wechsler, 1991). Verbal IQ (VIQ) was significantly different between the groups. Lower VIQ scores have been reported previously in children with dyslexia, and were not found to relate to degree of phonological deficits or functional imaging findings (Temple et al., 2001). Nevertheless, all subjects had intelligence within the average range.

Poor readers had a previous diagnosis of dyslexia made by a psychologist either privately or through a school district and a current Woodcock-Johnson-III (WJ-III; Woodcock, 2001) Basic Reading Composite (BRC) score equal to or below the 30th percentile. The BRC is an average of the Letter-Word Identification (WJ-LWID) and Word Attack (WJ-WA) subtests. These tests measure pronunciation accuracy during oral reading of single real words and pseudowords. We suspect that the relatively high reading scores in the children diagnosed with dyslexia may reflect the Palo Alto, California regional demographics, where many poor readers are exposed to enriched curricula and remediation programs. Subjects were also administered Passage Comprehension (WJ-PC), Reading Fluency (WJ-RF), and Spelling (WJ-SP) subtests from the WJ-III and the six core subtests from the Comprehensive Test of

TABLE I
Subject Characteristics

Subject Characteristics	Normal Readers (n=7)	Poor Readers (n=7)	Significance
Age	10.4 (1.9)	11.0 (0.7)	ns
Gender (% male)	86	86	ns
HQ	97.1 (7.6)	83.9 (23.3)	ns
SES (Hollingshead)	54.1 (13.14)	55.2 (12.9)	ns
VIQ	119.1 (6.3)	102.6 (14.9)	$p = .019$
PIQ	122.9 (14.9)	120.6 (21.0)	ns
FSIQ	122.9 (9.6)	111.7 (16.9)	ns
WJ-III Tests of Achievement			
WJ-LWID	108.3 (5.2)	85.0 (4.3)	$p < .001$
WJ-WA	108.3 (6.8)	93.3 (3.7)	$p < .001$
WJ-PC	102.9 (6.1)	88.3 (10.6)	$p = .008$
WJ-RF	117.7 (19.4)	89.4 (9.5)	$p = .005$
WJ-SP	111.3 (6.1)	82.7 (4.8)	$p < .001$
WJ-BRC	109.1 (6.4)	88.6 (3.2)	$p < .001$
CTOPP			
CTOPP-PA	105.6 (8.6)	90.6 (12.5)	$p = .023$
CTOPP-PM	109.0 (13.2)	92.3 (10.8)	$p = .023$
CTOPP-RN	111.0 (11.6)	86.6 (7.0)	$p < .001$

TABLE II
Correlations Among Behavioral Measures

	PIQ	WJ-LWID	WJ-WA	WJ-PC	WJ-RF	WJ-SP	CTOPP-PA	CTOPP-PM	CTOPP-RN
VIQ	.381	.701**	.691**	.822**	.696**	.644*	.654*	.607*	.613*
PIQ		.059	.302	.084	.478	.072	– .115	.050	.471
WJ-LWID			.886**	.762**	.797**	.937**	.673**	.685**	.689**
WJ-WA				.666**	.788**	.838**	.634*	.661*	.687**
WJ-PC					.696**	.747**	.523	.416	.473
WJ-RF						.743**	.499	.422	.764**
WJ-SP							.604*	.558*	.687**
CTOPP-PA								.611*	.504
CTOPP-PM									.491

** significant at $p < .001$ (2-tailed)
* significant at $p < .05$ (2-tailed)

Phonological Processing (CTOPP), (Wagner et al., 1997) in order to assess phonological awareness skills. These subtests produced Phonological Awareness (CTOPP-PA), Phonological Memory (CTOPP-PM) and Rapid Naming (CTOPP-RN) composite scores. Performances across reading, spelling, and phonological processing measures were moderately to strongly correlated for the entire group, as expected (Table II).

Among the poor readers, four of the seven had a discrepancy of at least one standard deviation between their VIQ and BRC. Only one of these subjects also exhibited a phonological awareness deficit (defined by a CTOPP-PA score of at least one standard deviation below the mean). Of the other three poor readers, two had phonological awareness deficits, one had a rapid naming deficit based on a CTOPP-RN score of at least one standard below the mean and one had a double deficit (Wolf et al., 1999). However, because of the small sample size all subsequent analyses were conducted with the entire group of poor readers.

MRI Acquisition Protocols

All images were acquired on 1.5T Signa LX (Signa CVi, GE Medical Systems, Milwaukee, WI) using a self-shielded, high performance gradient system capable of providing a maximum gradient strength of 40 mT/m at a gradient rise time of 268 μs for each of the gradient axes. For excitation and signal reception, we used a standard quadrature head coil provided by the vendor. Head motion was minimized by placing cushions around the head and securing a Velcro strap across the forehead. Children watched and listened to cartoons via a video projection system and Resonance Technologies pneumatic headphones during the scan to occupy their attention and to reduce anxiety.

Anatomical MRI

We collected high-resolution T1-weighted anatomical images. However, these images were not used for the analyses reported here, except to confirm the locations of the DTI measurements with respect to conventional brain landmarks where the EPI T2-weighted images (see below) were inconclusive.

Diffusion Imaging Protocol

The DTI protocol involved four three-minute whole-brain scans. These were averaged to improve

signal quality. The pulse sequence was a diffusion-weighted single-shot spin-echo, echo planar imaging sequence (TE = 63 ms; TR = 12s; FOV = 260 mm, and matrix size = 128 × 128, bandwidth = ± 110 kHz, partial *k*-space acquisition). Thirty-eight axial, 3 mm thick slices (no skip) were measured for two b-values, b = 0 and b = ~ 800 s/mm^2. The high b-value was obtained by applying gradients along 12 different diffusion directions. Two gradient axes were energized simultaneously to minimize TE: $G_0 = (0\ 0\ 0)^T$, $G_1 = 1/\sqrt{2}\ (1\ 1\ 0)^T$, $G_2 = 1/\sqrt{2}\ (1\ 0\ 1)^T$, $G_3 = 1/\sqrt{2}\ (0\ 1\ 1)$, $G_4 = 1/\sqrt{2}\ (-1\ 1\ 0)^T$, $G_5 = 1/\sqrt{2}\ (-1\ 0\ 1)^T$, and $G_6 = 1/\sqrt{2}\ (0\ -1\ 1)$. This pattern was repeated two times for each slice. The polarity of the effective diffusion-weighting gradients was reversed for odd repetitions to remove cross-terms between diffusion gradients and both imaging and background gradients.

Image Processing

DTI data were first pre-processed using a custom program based on normalized mutual information that removed eddy current distortion effects. These distortions in the raw diffusion-weighted images were corrected using a constrained non-rigid mutual information image registration (Bammer et al., 2001). The six elements of the diffusion tensor were determined by multivariate regression using matrix calculus on a per voxel basis (Basser, 1995; Basser et al., 1996). The geometric representation of the proton displacement front in anisotropic Gaussian diffusion is an ellipsoid. The orientation (eigenvectors) and magnitude (eigenvalues) of the principal axes of the diffusion tensor can be derived by means of eigenanalysis. The orientation of the eigenvector with the largest eigenvalue is assumed to run parallel to the axon. The fractional anisotropy (FA) is calculated using the three principal diffusivities and the mean diffusivity (Basser, 1995; Basser et al., 1996). The CI is computed by comparing the direction of the longest axis of the diffusion ellipsoid across a neighborhood of nine voxels. Specifically, the CI is the mean dot-product (also called inner product or scalar product) of the vector representing the longest axis of the diffusion ellipsoid within a voxel with that of each of its eight neighboring voxels. When these vectors are normalized to unit length, this value ranges from zero to one (Klingberg et al., 1999, 2000). The fiber direction is identified as the direction of the longest axis of the diffusion ellipsoid. It is commonly visualized using an RGB image where red, green and blue values represent the X, Y and Z coordinates of the principal vector. The DTI data were processed using custom MATLAB scripts (Mathworks, Sherborn, MA) and compiled C-code. The statistical analyses, reported below, were performed using SPM99 (Wellcome Department of Cognitive Neurology, London, UK).

For each subject, the T2-weighted images that were acquired as part of the EPI DTI sequence (b-value = 0) were spatially normalized to the MNI EPI template transforming them onto a MNI mean brain using 12 iterations of the non-linear spatial normalization algorithm. The images were resampled to 2 mm isotropic voxels using bilinear interpolation. Each normalized brain was visually inspected to insure accurate co-registration with the template. All coordinates listed below were transformed from the MNI template to Talairach coordinates. The FA and CI images were normalized to the same template by applying the parameters derived from the normalization of T2-weighted images. These images were also resampled to 2 mm isotropic voxels using bilinear interpolation. Care must be taken when normalizing diffusion tensor data. For the present analysis, we primarily were interested in two scalars computed from the diffusion tensor, FA and CI. Both FA and CI were computed for each individual subject before normalization. Since FA is computed for each voxel independently and is direction free, it would be completely unaffected by the normalization process. CI, on the other hand, measures the homogeneity of tensor direction across a neighborhood of voxels. While CI would be unaffected by affine transforms it is potentially affected by the non-linear stage of the normalization applied here. However, the SPM spatial normalization used here varies very slowly across the image volume compared to the size of the CI neighborhood. Hence, the CI value is nearly invariant when it is computed before or after the spatial normalization.

A white matter mask was created for each brain by processing the normalized T2-weighted images with the SPM99 segmentation algorithm. A voxel was marked as white matter if its white-matter probability was ≥ 80%. We computed a single white matter mask as the intersection of the white matter across all brains. Thus, all reported differences between the two groups are restricted to white matter regions common to all the normalized brains.

Several of the analyses investigating group differences and correlations were restricted to voxels in the temporo-parietal region using a predefined volume of interest (VOI) based on the previous reported adult study (Klingberg et al., 2000). The VOI was located within x = – 36 to – 26, y = – 50 to – 10, and z = 0 to 32 mm relative to the anterior commissure, and had a volume of 960 mm^3 (120 voxels). A comparable VOI was made to probe the analogous region in the right hemisphere. The intersection of the single white matter mask and the right and left VOI was used in all subsequent analyses.

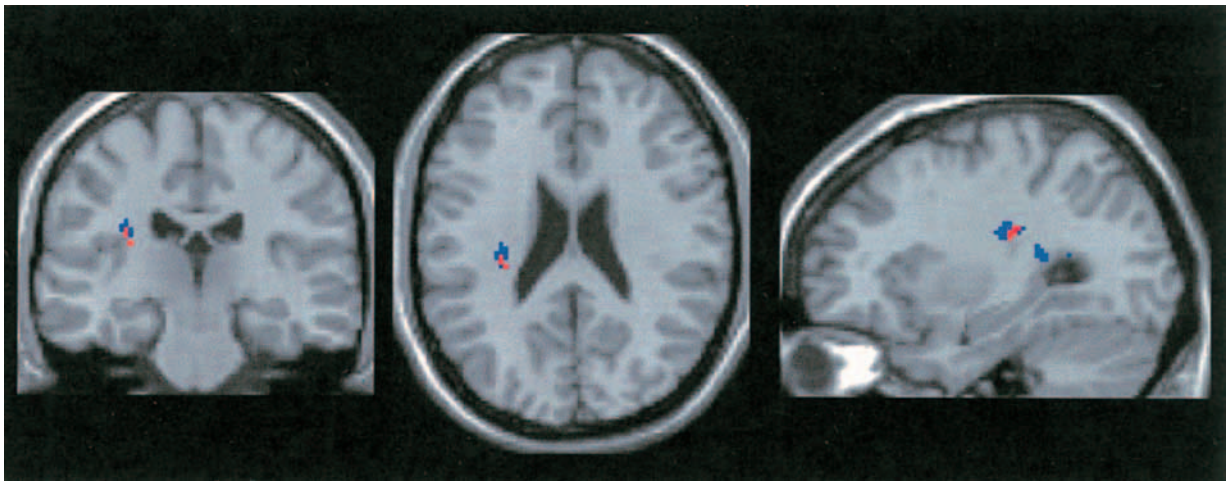

Fig. 1 – *Brain regions that showed significant differences in normal and poor reading children are presented. Left temporo-parietal regions are shown in three slices of the SPM99 T1 canonical brain. Red indicates voxels with significant group differences in FA and blue indicates voxels with significant differences in CI.*

Results

Group Differences (FA, CI, and T2-weighted)

Group differences in FA were analyzed with a one-way ANOVA using SPM99. Significant group differences in FA were found in a cluster of 14 voxels in the left temporo-parietal region (peak voxel p = .007, two-tailed, uncorrected) at Talairach coordinates (– 28 – 26 23) (Talairach et al., 1988). The mean FA values in this cluster were 0.51 (SE = 0.02) for the normal readers and 0.43 (SE = 0.01) for the poor readers, and, as expected, these mean FA values were significantly different (p = .003, two-tailed). The areas that showed these group differences are presented in Figure 1. Figure 2 is a three-dimensional rendering of one subject's left hemisphere that indicates the projection of this white matter region to the cortical surface.

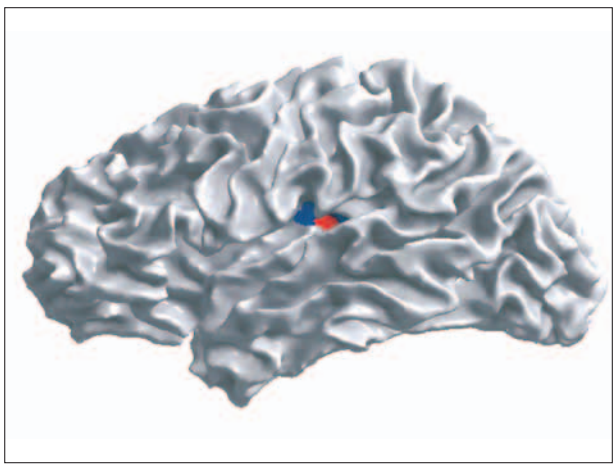

Fig. 2 – *Brain regions that showed significant differences in normal and poor reading children in a 3-D rendering of one subject's left hemisphere. The FA and CI white matter regions are projected to the cortical surface. The gray matter has been stripped away to facilitate visualization.*

In addition, there was a small cluster of five voxels with significant group differences in FA (p = .017, two-tailed uncorrected) at Talairach coordinates (28 – 45 28) within the right hemisphere VOI. The FA values did not correlate with any behavioral measures and further analyses, therefore, were limited to the left hemisphere VOI.

Group differences in CI were analyzed using a similar procedure. Significant group differences in CI were found in two clusters of voxels in the left temporo-parietal region. The first cluster consisted of 31 voxels with the peak at Talairach coordinates (– 32 – 20 23) (p = .001, two-tailed, uncorrected) and the second cluster consisted of 35 voxels with the peak at (– 28 – 32 22) (p = .003, two-tailed, uncorrected). These two clusters surrounded the region identified by the FA group analyses (see Figure 1). There were significant differences in the mean CI values of these voxels between the normal (Mean = 0.77; SE = 0.09) and poor readers (Mean = 0.70; SE = 0.10; p < .001).

Individual Brains

Using the inverse of the SPM99 normalization transformation matrix, all the MNI coordinates in the FA cluster were identified in each subject's unnormalized T2-weighted brain. Visual examination of these images indicated that the coordinates all fell within white matter tracts away from the white matter / gray matter border or white matter / CSF border. As we describe above, had the significant voxels fallen on the white / gray or white / CSF border, we would be concerned that the significance was due to unmodeled random errors in the white matter segmentation and the spatial normalization procedure. By checking the position of the significant locations within each brain, we confirmed that the significant voxels in the normalized data fell well within the white

matter of each individual brain and in the same approximate anatomical region across all subjects.

Correlation with Behavioral Measures

The mean FA value of the left temporo-parietal cluster significantly correlated with WJ-LWID (r = .62; p = .017), WJ-WA (r = .59; p = .026), WJ-SP (r = .66; p = .010) and CTOPP-RN (r = .65; p = .011) accounting for 35% to 44% of the variance across these measures for the entire group. The WJ-BRC significantly correlated with the mean FA value of this cluster (r = .62, p = .019) for the entire group (see Figure 3). Interestingly the FA did not correlate with CTOPP-PA (r = .072). In addition the mean FA value was not significantly correlated with age (r = -.072), HQ (r = .122), VIQ (r = .352), or PIQ (r = .232).

The mean CI value of the significant voxels in the left temporo-parietal region also significantly correlated with WJ-LWID (r = .75; p = .002), WJ-WA (r = .69; p = .006), WJ-SP (r = .71; p = .004), and CTOPP-RN (.74; p = .002) accounting for 48% to 57% of the variance across these measures for the entire group. The BRC significantly correlated with the mean CI value (r = .75; p = .002) for the entire group (see Figure 4). Similar to the mean FA value, the mean CI value was not significantly correlated with age (r = -.280), HQ (r = .115), VIQ (r = .334), PIQ (r = .237), or CTOPP-PA (r = .169).

The principal diffusion direction (presumably indicative of the primary axonal orientation within a voxel) was computed from the DTI data for both groups of children. Across all subjects, 74% of the voxels in the significant cluster (88% normal reading children; 61% poor reading children) were oriented in the inferior-superior direction. This difference almost reached significance [t (12) = 2.12, p = .056, two-tailed]. In addition, for the poor reading children, 28% of the voxels were oriented in the anterior-posterior direction compared to 7% for the normal reading children [t (12) = – 1.71, p = .112, two-tailed]. For both groups of children there were only a very small number of fibers oriented in the left-right direction (5% normal reading children, 1% poor reading children) [t (12) = – 0.63, p = .539, two-tailed]. Principal diffusion direction maps for both groups are presented in Figure 5. The data shown in Figure 5 are averaged across subjects. The principal diffusion vectors were adjusted to account for the affine rotation component of the normalization procedure. The non-linear warping component of the normalization did not influence these conclusions as verified by transforming the significant cluster of voxels back to each individual (unnormalized) brain.

Most of the analyses reported here were restricted to the left temporo-parietal region that had been identified in a previous adult study (Klingberg et al., 2000). In this study, we

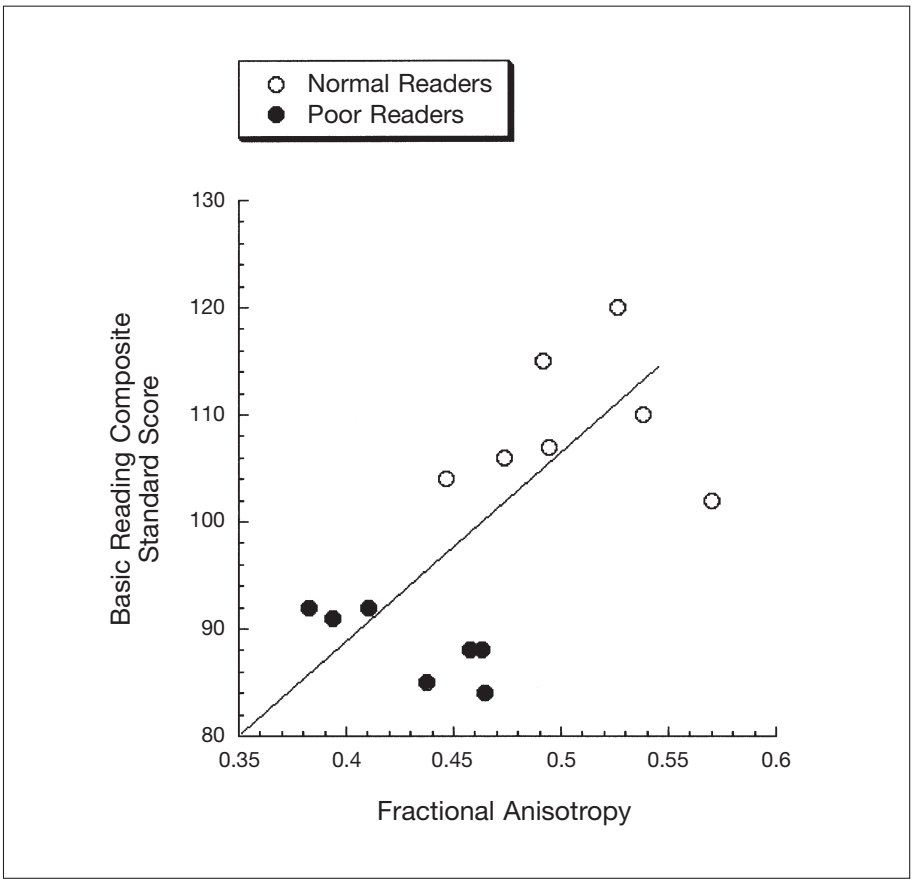

Fig. 3 – *Scatter plot showing the correlation between the mean FA, across 14 significant voxels, and the BRC score (r = .62, p = .019).*

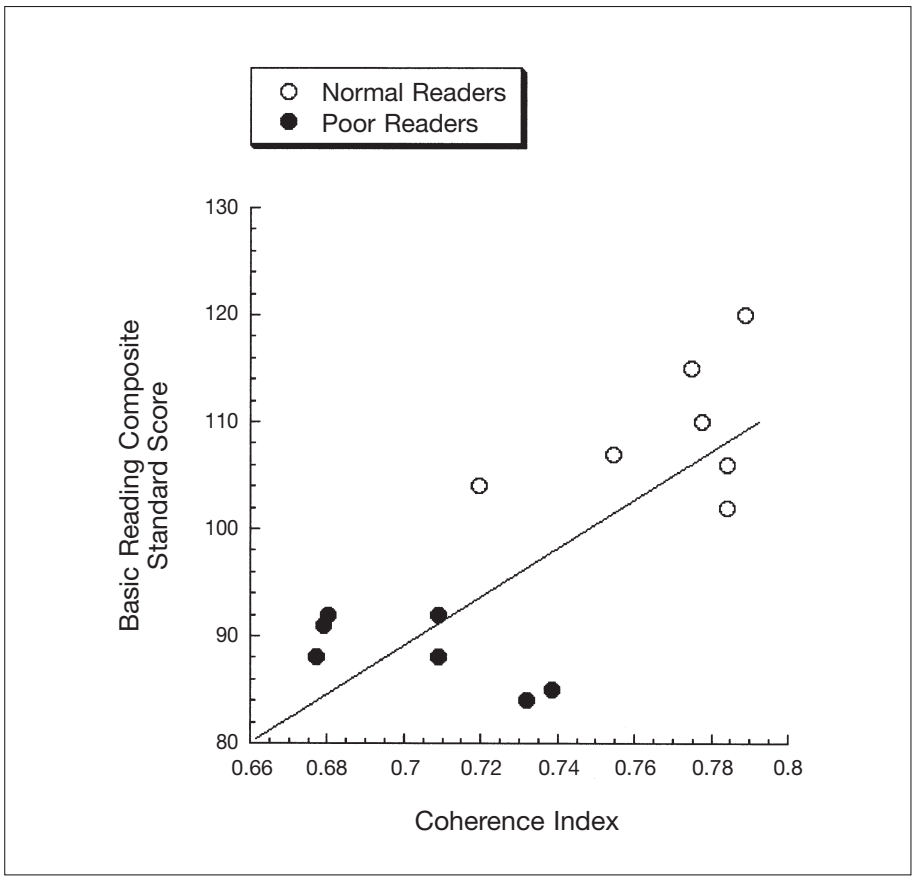

Fig. 4 – *Scatter plot showing the correlation between the mean CI, across 66 significant voxels, and the BRC score (r = .75, p = .002).*

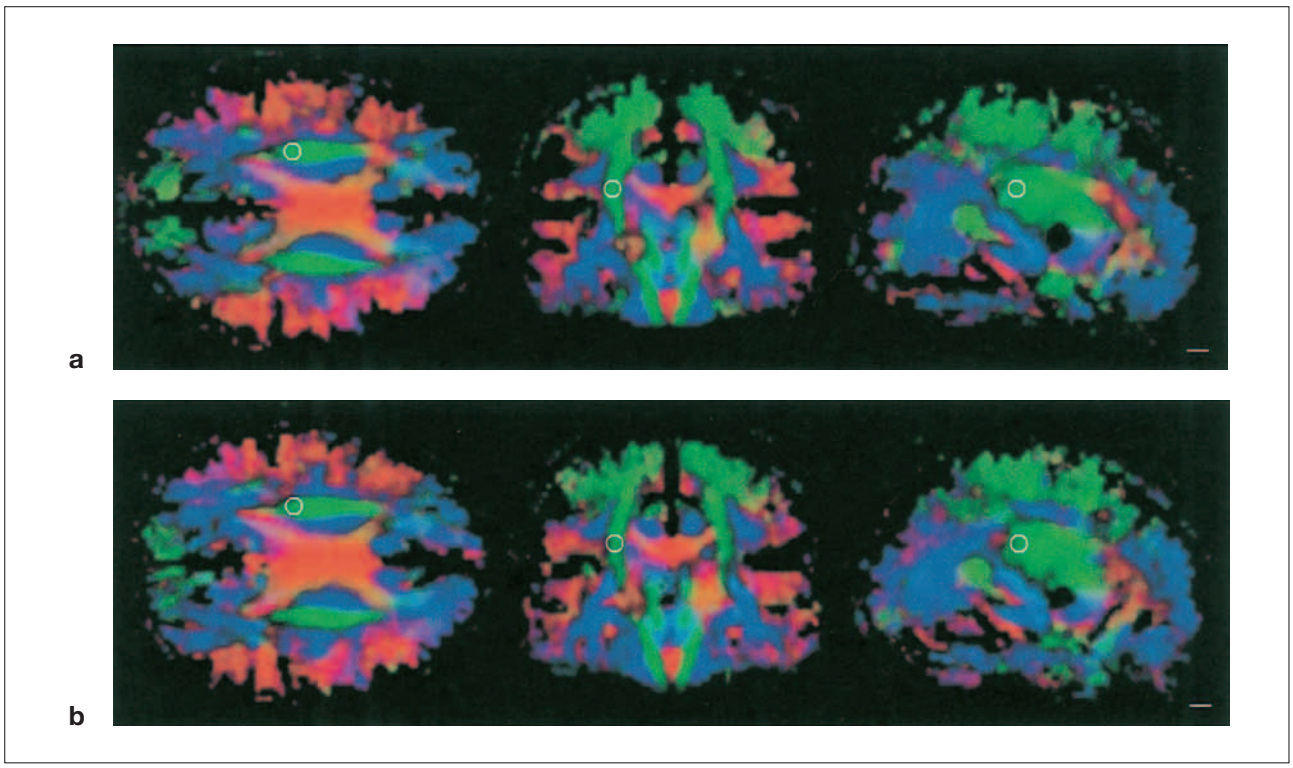

Fig. 5 – *Color maps indicating the principal diffusion direction in three orthogonal slices in the normal reading group (a) and the poor reading group (b). The white circle indicates the center of the cluster of voxels that were correlated with reading. In this representation, voxels with a principal diffusion direction oriented left-right are red, those with an anterior-posterior orientation are blue and those oriented inferior-superior are green. Voxels with intermediate directions are represented by intermediate colors (e.g., a voxel intermediate between anterior-posterior and inferior-superior are green + blue = cyan). The axial slice (left) is at Talairach Z = 24 mm, the coronal slice (center) is at Talairach Y = – 26 mm and the sagittal slice (right) is at Talairach X = – 28 mm. The scale bar is 1 cm.*

specifically wished to examine whether the differences that had been observed in adult white matter structure were present in individuals with poor reading performance at much younger ages. However, in our exploration of the data, we also analyzed the whole brain to see whether FA and CI in other regions differed significantly between the two groups of readers. We found a difference in FA in left frontal cortex in a cluster of 20 voxels at Talairach coordinates (– 22 21 23) and for CI in a cluster of 30 voxels at Talairach coordinates (– 22 18 12). The mean FA and CI values correlated with reading-related tasks. We do not mean to imply, that there are no other differences; only that these differences were outside the reach of the methods and statistical power of this study.

Discussion

Normal and poor readers differ in both FA and CI indicators of white matter structure in a left temporo-parietal region of the brain. These same white matter indicators correlated with multiple aspects of reading performance, including measures of word reading, spelling, and rapid naming. This region was also associated with reading ability in adults. The presence of these white matter differences at early ages suggests, but does not prove, that these differences may be one cause of poor reading, rather than a consequence of poor reading over a lifetime. This report shows an association in the structure of white matter and a specific cognitive ability in healthy children.

The main results of this study extend Klingberg's findings in adults (2000) to children. However, the effect sizes in the present study are not as strong as those of Klingberg, even though the methods and sample sizes are similar. The smaller effect size in our sample of children could be due to sampling differences- both studies have relatively small sample sizes, so we would expect low power and biased samples. However, the smaller effect size in children may be real and thus indicative of a developmental effect. For example, if this area in the left temporo-parietal region is continuing to develop, its location may be more variable across children because they have had fewer years of reading experience than adults. Additionally in this study, we spatially normalized the children's brains to a standard adult brain template using normalization techniques that were developed for adult brains. Although this technique has been validated in prior functional imaging studies with children greater than 6 years of age (Kaplan et al., 1997; Muzik et al., 2000; Burgund et al., 2002), it could introduce greater error variance (Poldrack et al., 2002). This variability in the location of specific anatomical regions and the overall size of the children's brains could have contributed to the weaker effects observed in the present study compared to the previous adult study.

In preliminary data with eight normal reading adult subjects, using similar methods, we found that the adult FA values in this brain region follow the same general trend: reading performance correlates with FA. The normal adult reading group included individuals of average or slightly below average reading scores whose FA was in the same range as the dyslexic children. Consequently, the FA value may be more useful for predicting average or better reading performance than diagnosing reading dysfunction.

The observed differences in FA and CI between normal and poor readers can be explained by any of several anatomical differences. High FA and high CI in a voxel indicate the presence of a major fiber tract of dense, myelinated axons oriented in a common direction. However, low FA and CI may be the result of reduction in density, myelination or directional coherence. Klingberg et al. (2000) interpreted their results as a microstructural (myelination or axonal density) difference between good and poor readers, and this is a plausible interpretation of our results.

However, analysis of the principal diffusion direction data may suggest a different interpretation. We found evidence that the two groups of children varied with regard to their principal diffusion direction in the region that showed the FA difference. Although not statistically significant, there was a trend indicating that more voxels were oriented in the inferior-superior direction for the normal reading children compared to the poor reading children. For the poor reading children, about 28% of the voxels were oriented in the anterior-posterior direction. Based on this interpretation, the differences reflected in FA and CI measurements may be due to differences between the groups in fiber tract sizes or in structural differences in the region where several major tracts meet (Mori et al., 2002). Unfortunately it is not possible to distinguish between these two interpretations based on the results of the current study.

Regardless of the interpretation of the group differences in FA and CI, we can use the principal diffusion direction data to help determine which of the major white matter fiber tracts pass through this region. Across both groups of children, the majority of voxels in this white matter region were oriented along the superior-inferior axis (see Figure 5). This orientation, along with the gross position, suggests that this region lies at the border between the superior longitudinal (arcuate) fasciculus (SLF) and projection fibers (corona radiata). The SLF is interesting because this major fiber tract includes a subdivision (the arcuate fasciculus) that is known to connect Broca's and Wernicke's areas. Lesions along this pathway often result in aphasia. If the region is in fact in the SLF, then the inferior-superior orientation suggests that it is part of the

SLF branch that curves downwards as it projects to the temporal lobe, although we cannot rule out the possibility these are projection fibers. We are currently pursuing fiber tracing analyses to help resolve this question.

The strong inferior-superior orientation in our data is different from the bias toward anterior-posterior orientation reported in Klingberg et al. (2000). The region they reported was much larger than ours and probably included several different tracts (T. Klingberg, personal communication, June 7, 2003). It may be that the region estimated in the present results overlaps with only the most superior part of their region.

The previous report of the relationship between DTI and reading in adults did not include other relevant measures, such as spelling and rapid naming. In addition to the relationships between measures of DTI and reading, we found that rapid naming correlated with both FA and CI. This lends more weight to the notion that time-sensitive processing may be facilitated by increased connectivity, as rapid naming is a timed measure of automaticity of information retrieval. Thus, areas of increased anisotropy, axonal organization, and fiber coherence may contribute to improved processing efficiency.

Our results suggest that the white matter microstructure and/or the macrostructural properties of major fiber tracts in this region of the brain are important for reading and spelling abilities. The stronger effects found in the previous adult study suggest that this effect may increase over time with reading experience. Further research is needed to gain a more precise understanding of the nature of these white matter differences. For example, a longitudinal study that measures the white matter structure in this regions would help illuminate how it relates to development and the acquisition of cognitive abilities. Significant changes take place in frontal networks at ages 3-6 years and both axon diameter and myelin sheath grow rapidly from birth until 2 years of age. However, it is not known how it continues to grow during adolescence and adulthood, although there is some indication that it does (Benes, 1998; Schmithorst et al., 2002). Strong anterior-posterior patterns of callosal development have also been reported (Thompson et al., 2000). Peak growth rates in fibers connecting sensory-reading cortex takes place from 8-11 years, attenuating after puberty. Specifically, the section of the corpus callosum which connects cortical regions in and near the language areas can increase in size by as much as eighty percent in the years prior to puberty. This change may be due to increased myelination or additional axonal migration; but either way, this is a substantial effect. This growth is accompanied by significant size increases in the temporal, parietal and occipital lobes and is one of the key reasons for aggressively pursuing measurements of functional development in these regions and relating the functional and anatomical development to the acquisition of skilled reading.

Acknowledgments: We thank S. Whitfield for her assistance in the analysis. This research was supported by grants from the Schwab Foundation for Learning and the NIH (EY 015000).

References

Adams M. *Beginning to Read*. Cambridge, MA: MIT Press, 1990.

Bammer R and Auer M. Correction of eddy-current induced image warping in diffusion-weighted single-shot EPI using constrained non-rigid mutual information image registration. *Paper presented at the meeting of the International Society of Magnetic Resonance in Medicine,* Glasgow, 2001.

Bammer R, Auer M, Keeling SL, Augustin M, Stables LA, Prokesch RW, Stollberger R, Moseley ME and Fazekas F. Diffusion tensor imaging using single-shot SENSE-EPI. *Magnetic Resonance in Medicine, 48:* 128-136, 2002.

Basser PJ. Inferring microstructural features and the physiological state of tissues from diffusion-weighted images. *Nuclear Magnetic Resonance in Biomedicine, 8:* 333-344, 1995.

Basser PJ and Pierpaoli C. Microstructural and physiological features of tissues elucidated by quantitative-diffusion-tensor MRI. *Journal of Magnetic Resonance Series B, 111:* 209-219, 1996.

Benes FM. Brain development, VII. Human brain growth spans decades. *The American Journal of Psychiatry, 155:* 1489, 1998.

Brunswick N, McCrory E, Price CJ, Frith CD and Frith U. Explicit and implicit processing of words and pseudowords by adult developmental dyslexics: A search for Wernicke's Wortschatz? *Brain, 122:* 1901-1917, 1999.

Burgund ED, Kang HC, Kelly JE, Buckner RL, Snyder AZ, Petersen SE and Schlaggar BL. The feasibility of a common stereotactic space for children and adults in fMRI studies of development. *Neuroimage, 17:* 184-200, 2002.

Galaburda AM, Sherman GF, Rosen GD, Aboitiz F and Geschwind N. Developmental dyslexia: Four consecutive patients with cortical anomalies. *Annals of Neurology, 18:* 222-233, 1985.

Grigorenko EL. Developmental dyslexia: An update on genes, brains, and environments. *Journal of Child Psychology and Psychiatry, and Allied Disciplines, 42:* 91-125, 2001.

Habib M. The neurological basis of developmental dyslexia: An overview and working hypothesis. *Brain, 123:* 2373-2399, 2000.

Hollingshead A. *Four Factor Index of Social Skills*. New Haven: Yale University, 1975.

Hunsche S, Moseley ME, Stoeter P and Hedehus M. Diffusion-tensor MR imaging at 1.5 and 3.0 T: Initial observations. *Radiology, 221:* 550-556, 2001.

Kaplan DM, Liu AM, Abrams MT, Warsofsky IS, Kates WR, White CD, Kaufmann WE and Reiss AL. Application of an automated parcellation method to the analysis of pediatric brain volumes. *Psychiatry Research, 76:* 15-27, 1997.

Klingberg T, Hedehus M, Temple E, Salz T, Gabrieli JD, Moseley ME and Poldrack RA. Microstructure of temporo-parietal white matter as a basis for reading ability: Evidence from diffusion tensor magnetic resonance imaging. *Neuron, 25:* 493-500, 2000.

Klingberg T, Vaidya CJ, Gabrieli JD, Moseley ME and Hedehus M. Myelination and organization of the frontal white matter in children: A diffusion tensor MRI study. *Neuroreport, 10:* 2817-2821, 1999.

Le Bihan D, Mangin JF, Poupon C, Clark CA, Pappata S, Molko N and Chabriat H. Diffusion tensor imaging: Concepts and applications. *Journal of Magnetic Resonance Imaging, 13:* 534-546, 2001.

Mori S, Kaufmann WE, Davatzikos C, Stieltjes B, Amodei L, Fredericksen K, Pearlson GD, Melhem ER, Solaiyappan M, Raymond GV, Moser HW and van Zijl PC. Imaging cortical association tracts in the human brain using diffusion-tensor-based axonal tracking. *Magnetic Resonance in Medicine, 47:* 215-223., 2002.

Muzik O, Chugani DC, Juhasz C, Shen C and Chugani HT. Statistical parametric mapping: Assessment of application in children. *Neuroimage, 12:* 538-549, 2000.

OLDFIELD RC. The assessment and analysis of handedness: The Edinburgh inventory. *Neuropsychologia, 9:* 97-113, 1971.

PAULESU E, DEMONET JF, FAZIO F, MCCRORY E, CHANOINE V, BRUNSWICK N, CAPPA SF, COSSU G, HABIB M, FRITH CD and FRITH U. Dyslexia: Cultural diversity and biological unity. *Science, 291:* 2165-2167, 2001.

PAULESU E, FRITH U, SNOWLING M, GALLAGHER A, MORTON J, FRACKOWIAK RS and FRITH CD. Is developmental dyslexia a disconnection syndrome? Evidence from PET scanning. *Brain, 119:* 143-157, 1996.

POLDRACK RA, PARE-BLAGOEV EJ and GRANT PE. Pediatric functional magnetic resonance imaging: Progress and challenges. *Topics in Magnetic Resonance Imaging, 13:* 61-70, 2002.

RUMSEY JM. The biology of developmental dyslexia. *The Journal of the American Medical Association, 268:* 912-915, 1992.

RUMSEY JM, NACE K, DONOHUE B, WISE D, MAISOG JM and ANDREASON P. A positron emission tomographic study of impaired word recognition and phonological processing in dyslexic men. *Archives of Neurology, 54:* 562-573, 1997.

SCHMITHORST VJ, WILKE M, DARDZINSKI BJ and HOLLAND SK. Correlation of white matter diffusivity and anisotropy with age during childhood and adolescence: A cross-sectional diffusion-tensor MR imaging study. *Radiology, 222:* 212-218, 2002.

SHAYWITZ BA, SHAYWITZ SE, PUGH KR, MENCL WE, FULBRIGHT RK, SKUDLARSKI P, CONSTABLE RT, MARCHIONE KE, FLETCHER JM, LYON GR and GORE JC. Disruption of posterior brain systems for reading in children with developmental dyslexia. *Biological Psychiatry, 52:* 101-110, 2002.

SHAYWITZ SE. Dyslexia. *The New England Journal of Medicine, 338:* 307-312, 1998.

SHAYWITZ SE, SHAYWITZ BA, PUGH KR, FULBRIGHT RK, CONSTABLE RT, MENCL WE, SHANKWEILER DP, LIBERMAN AM, SKUDLARSKI P, FLETCHER JM, KATZ L, MARCHIONE KE, LACADIE C, GATENBY C and GORE JC. Functional disruption in the organization of the brain for reading in dyslexia. *Proceedings of the National Academy of Sciences of the United States of America, 95:* 2636-2641, 1998.

SIMOS PG, BREIER JI, FLETCHER JM, BERGMAN E and PAPANICOLAOU AC. Cerebral mechanisms involved in word reading in dyslexic children: A magnetic source imaging approach. *Cerebral Cortex, 10:* 809-816, 2000a.

SIMOS PG, BREIER JI, FLETCHER JM, FOORMAN BR, BERGMAN E, FISHBECK K and PAPANICOLAOU AC. Brain activation profiles in dyslexic children during non-word reading: A magnetic source imaging study. *Neuroscience Letters, 290:* 61-65, 2000b.

STEIN J. The magnocellular theory of developmental dyslexia. *Dyslexia, 7:* 12-36, 2001.

TALAIRACH J and TOURNOUX P. *Co-Planar Stereotaxic Atlas of the Human Brain*: Thieme Medical Publishers, 1988.

TEMPLE E. Brain mechanisms in normal and dyslexic readers. *Current Opinions in Neurobiology, 12:* 178-183, 2002.

TEMPLE E, POLDRACK RA, SALIDIS J, DEUTSCH GK, TALLAL P, MERZENICH MM and GABRIELI JD. Disrupted neural responses to phonological and orthographic processing in dyslexic children: An fMRI study. *Neuroreport, 12:* 299-307, 2001.

THOMPSON PM, GIEDD JN, WOODS RP, MACDONALD D, EVANS AC and TOGA AW. Growth patterns in the developing brain detected by using continuum mechanical tensor maps. *Nature, 404:* 190-193, 2000.

WAGNER RK, TORGESEN JK and RASHOTTE CA. *Comprehensive Test of Phonological Processing.* Austin, TX: Pro-Ed, Inc., 1997.

WECHSLER D. *Wechsler Intelligence Scale for Children-Third Edition.* San Antonio, TX: The Psychological Corporation, 1991.

WOLF M and BOWERS P. The double-deficit hypothesis for the developmental dyslexias. *Journal of Educational Psychology, 91:* 415-438, 1999.

WOODCOCK RW, MCGREW, K.S., MATHER, N. *Woodcock-Johnson-III Tests of Achievement.* Itasca, IL: Riverside Publishing, 2001.

Gayle K. Deutsch, Ph.D., Stanford University, Department of Psychology, Jordan Hall, Building 420, Stanford, CA 94305. e-mail: gdeutsch@stanford.edu